



# Conversion Characteristics of Alternative Reducing Agents for the Bath Smelting Processes in an Oxidizing Atmosphere

Samira Lotfian<sup>1</sup> · Hesham Ahmed<sup>1,3</sup> · Kentaro Umeki<sup>2</sup> · Caisa Samuelsson<sup>1</sup>

Received: 27 November 2018 / Accepted: 7 February 2019 / Published online: 28 February 2019  
© The Author(s) 2019

## Abstract

The amount of plastic-containing materials, such as shredder residue material, which is generated after the processing of electronic equipment waste, is increasing. One interesting option for the sustainable management of these materials, instead of incineration or landfilling, is recycling through injection in a bath smelting process, such as zinc fuming. In this way, the plastic material could partially substitute coal as a reductant in the process. In such processes, shredder residue material is injected alongside air into the furnace at temperatures up to 1250 °C. Once the material is injected, it undergoes several conversion steps, including ignition, devolatilization, and char oxidation. In this study, the conversions of shredder residue material and other pure plastic materials were investigated using a drop tube furnace and an optical single-particle burner. The effect of particle size on the conversion time of each material was studied. The conversion time of the particles increases as the particle size increases, although the relationship is not linear. The results indicate that plastic materials with a particle size range of 1–7 mm have a considerably longer conversion time than that of coal used in the conventional processes.

**Keywords** Shredder residue materials · Thermal conversion · Oxidizing conditions · Drop tube furnace · Optical single-particle burner

## Introduction

The production of electric and electronic equipment (EEE) is a fast-growing area. This development has resulted in an increase of waste electric and electronic equipment (WEEE) [1]. Shredder residue material (SRM), which is a residue generated during the shredding of WEEE, contains metals, metal oxides, and a high fraction of plastic material. Recycling of these residue materials is challenging, as it is heterogeneous; just the plastic fraction could consist of more

than 15 different plastic types [2]. Instead of the current available options of landfilling and incineration, utilization as a reductant in the smelting processes is a more promising option [3].

Utilization of SRM in the smelting process provides a promising route for their recycling, since both the organic and nonorganic parts can be recycled. One example of the smelting processes is zinc fuming, which involves the reduction of zinc oxide from zinc-containing slag by the injection of a reducing agent and air. Traditionally, coal is used as a reducing agent in this process. However, the utilization of plastic-containing materials such as shredder residue material is possible [4]. There are several studies available on the behavior of coal in the zinc fuming process. G. G. Richard et al. [5] extensively studied the zinc fuming process and the behavior of coal in the furnace. The result of the tuyere back-pressure measurement indicates that the coal and air injected will be discharged into the furnace as a continuous series of bubbles. This series of bubbles can directly rise up the furnace wall, which is called a tuyere gas stream. A fraction of the injected coal will combust in the tuyere gas stream. Another fraction of coal that did not fully combust in the tuyere gas stream can be entrained in the slag.

---

The contributing editor for this article was Bart Blanpain.

---

✉ Samira Lotfian  
samira.lotfian@ltu.se

<sup>1</sup> Department of Civil, Environmental and Natural Resources Engineering, Process Metallurgy, Minerals and Metallurgical Engineering, Luleå University of Technology, 971 87, Luleå, Sweden

<sup>2</sup> Department of Engineering Sciences and Mathematics, Energy Science, Energy Engineering, Luleå University of Technology, 971 87, Luleå, Sweden

<sup>3</sup> Central Metallurgical Research and Development Institute (CMRDI), Cairo, Egypt

The entrained coal particles will devolatilize and generate a bubble containing CO, CO<sub>2</sub>, H<sub>2</sub>, and H<sub>2</sub>O. CO and H<sub>2</sub> will reduce the oxides in the slag and produce CO<sub>2</sub> and H<sub>2</sub>O, which will react with the fixed carbon in char through the Boudouard reaction. The formed bubble will rise with the slag flow, and the extent of reduction in the process depends on the residence time of the formed bubble in the slag. Thus, for a reductant that is entrained in the slag to be efficient, the time needed for a particle to totally convert shall be shorter than the residence time of the formed bubble.

In another study, Huda et al. [6] made a computational fluid dynamic model of one of the zinc fuming furnaces that Richard used in his study. In contrast to Richard, their findings showed that the entrained coal particles seem to have less influence on the overall fuming. The results of the simulation predict that the major portion of the injected coal is combusted in the tuyere gas column. Furthermore, the products of combustion (CO, CO<sub>2</sub>, and H<sub>2</sub>O) are predicted to be present in the tuyere gas column and the gas–liquid emulsion zone around the column. The presence of CO at the gas–liquid interface reduces the ZnO present in the slag phase. Regardless of which phenomenon is controlling the process, both studies show the importance of the conversion characteristics of the reductant in the process. There are several experimental data on the conversion time of coal particles under oxidizing conditions, which are similar to the conditions in the fuming process. However, there is a lack of similar studies in the literature for plastic material and SRM. In order to consider these materials as alternative reducing agents, the ignition and combustion times need to be studied, as only limited literature studies are available.

The conversion time of coal with a particle size of 74 μm injected into a heated enclosure indicates that the ignition times for the particles is in the order of 30 ms [7]. In another study, McLean et al. [8] studied the conversion of single coal particles with a size of 65 μm in a particle burner with rapid heating. Ignition of the particle starts at 10 ms, and 25 ms after ignition, the particle was totally converted. Previous studies on the conversion characteristics of plastic-containing materials [9–13] including SRM [14, 15] are more related to the compositions of released volatiles, rather than conversion times. Therefore, the aim of this study is to determine the conversion time with rapid heating rates under oxidizing conditions. The conversion time is studied using two methods: an optical single-particle burner and a drop tube furnace. In the first method, the effect of particle size on conversion at two residence times is studied by measuring the solid residue yield. In the other method, continuous recording using a high-speed camera is used to identify the conversion characteristics and the conversion times under the studied conditions.

## Materials and Methods

In this study, two pure plastic materials—polyethylene (PE), polyurethane (PUR)—and one SRM were evaluated in addition to the bituminous coal. Two different colors of PE particles were tested: one PE is from a recycling fraction defined as black in color, and the other is from a production fraction and defined as transparent. PUR samples were in extruded form. Plastic materials were crushed using a rotary knife mill to different particle sizes of 1, 3, 5, and 7 mm. Experiments were repeated 20 times for the SRM to determine the average conversion time of the particles, as the material is heterogeneous. The coal sample particle size used in this study was 38 μm, which is similar to the particle size of coal that is used in conventional fuming processes. The ultimate and proximate analyses<sup>1</sup> of samples were determined by the certified laboratory, ALS Scandinavia AB, Sweden and are presented in Table 1.

### Drop Tube Furnace (DTF)

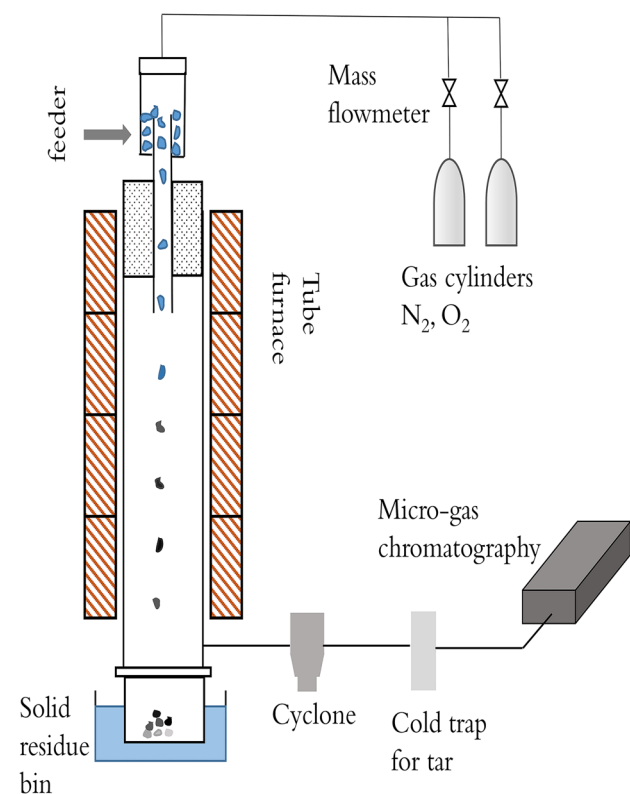
The first set of conversion experiments were carried out in a laminar-flow drop tube furnace at 1250 °C under atmospheres of N<sub>2</sub> and O<sub>2</sub> at a flow rate of 3 l/min (80% N<sub>2</sub>, 20% O<sub>2</sub>). The reactor consisted of an alumina tube (inner diameter: 54 mm) heated by six heating compartments with independent temperature controls, and is shown in Fig. 1. The detailed description of the furnace is reported elsewhere [16]. The gas-flow rate into the reactor was regulated by mass flow controllers (Bronkhorst: EL-FLOW series). The feeding system is based on a syringe pump that displaces a bed of particles upward, which eventually falls into the reactor through a hole in its middle. Vibration was applied to the feeding unit in order to improve the consistency of the feeding rate. The details of the injection system are found elsewhere [17]. Plastic particles fell directly into the high-temperature zone of the reactor through a water-cooled nozzle.

Primary gas (0.8 l/min of N<sub>2</sub> and O<sub>2</sub>) carried the plastic particles into the reactor while a secondary gas (2.2 l/min) was concentrically supplied to set the gas composition of the reactor. Both primary and secondary gases were at standard pressure and temperature. The ratio of N<sub>2</sub> to O<sub>2</sub> was 80/20 for both the primary and secondary gases. To study the effect of the particle's residence time on the extent of

<sup>1</sup> Standards for proximate analysis of coal: Moisture SS 187,155, ash SS 185,157, volatile SS-ISO 562:2010. Standards for proximate analysis of SRM: Moisture SS-EN 14,774:2009, ash SS-EN 14,775:2009, and volatile SS-EN 15,148:2009. Fixed carbon was calculated. Ultimate analysis standards for coal: CHN ASTM D5373, sulfur SS 187,177, and oxygen were calculated. Ultimate analysis standards for SRM: CHN SS-EN 15,104:2011, and oxygen were calculated.

**Table 1** Ultimate and proximate analyses of coal and plastic materials

	C (wt%)	H (wt%)	N (wt%)	S (wt%)	O (wt%)
Ultimate analysis					
Coal	84.0	4.8	1.3	0.30	5.2
SRM	57.3	6.1	1.4	0.16	12.9
PE	78.5	11.6	–	0.06	1.6
PUR	61.7	6.2	6.0	0.03	15.3
	Moisture (wt%)	Volatile (wt%)	Fixed carbon (wt%)	Ash (wt%)	
Proximate analysis					
Coal	0.8	26.5	68.3	4.4	
SRM	8.0	67.3	2.6	22.1	
PE	0.3	89.1	2.3	8.3	
PUR	1.6	80.8	7.1	10.5	

**Fig. 1** Schematic illustration of the laminar DTF, adapted from [16] (Color figure online)

conversion, two different furnace heights were used. One set of experiments was completed using the furnace with three compartments, and another set with six compartments. The total heated length of the furnace with six compartments was 2.3 m. To simplify the calculation, it is assumed that drag force and gas velocity do not affect the velocity of the falling particles. Thus, the residence time of the particles is calculated assuming free fall, using the following formula:

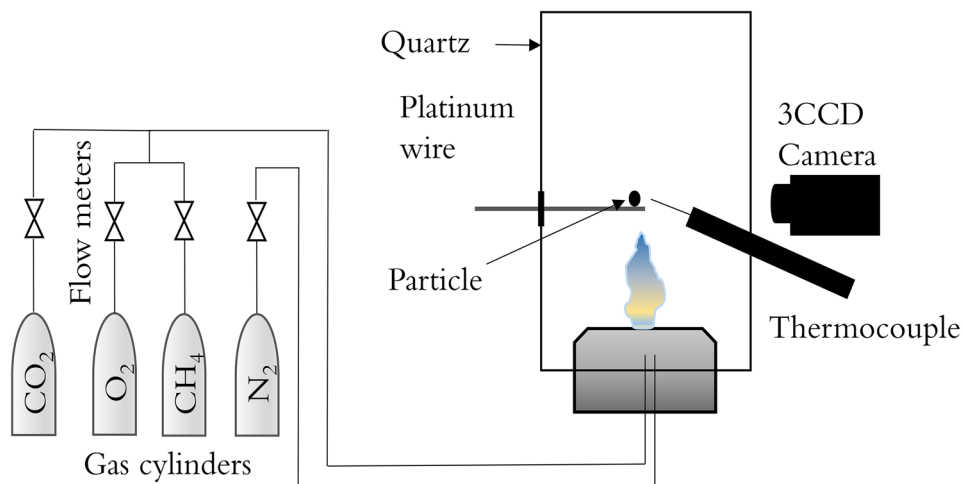
$$t = \sqrt{\frac{h \times 2}{g}}$$

where  $h$  (m) is the height of the furnace, and  $g$  ( $\text{m/s}^2$ ) is the gravitational constant. Therefore, the residence time is dependent on the height of the furnace, not the particle size. The calculated residence times were 0.47 and 0.65 s for the furnace with three and six compartments, respectively. The product of combustion consists of a solid residue, which falls into a water-cooled char bin.

### Optical Single-Particle Burner (OSB)

Another set of conversion experiments was carried out with an optical single-particle burner. A stable flame at the bottom was provided by a premixed combustion of  $\text{CH}_4$  in a small diameter McKenna burner (Holthuis & Associates). The temperature of the flame was controlled by the ratio of  $\text{CH}_4$ ,  $\text{CO}_2$ , and  $\text{O}_2$ . Flow rates of  $\text{CH}_4$ ,  $\text{O}_2$ ,  $\text{CO}_2$ , and  $\text{N}_2$  were controlled and measured by thermal mass-flow meters (MASS-VIEW series, Bronkhorst high-tech B.V.). The temperature of the combustion gas, which was measured a few mm from the particles, was set to 1250 °C. An  $\text{N}_2$  stream was supplied surrounding the flame at the same gas velocity as the  $\text{CH}_4/\text{O}_2$  mixture at standard state (200 mm/s). The flow rates of  $\text{CH}_4$ ,  $\text{O}_2$ , and  $\text{N}_2$  were 1.60, 3.21, and 5.79 l/min, respectively, and the ratio of  $\text{CO}_2/\text{N}_2$  was set to 1. A cylindrical tube with quartz windows and a sample-inserted port was used to stabilize the flow of combustion gas and  $\text{N}_2$ . Gas temperatures were measured by a thin wire thermocouple (diameter: 100  $\mu\text{m}$ ). Prior to the experiment, samples were placed on a platinum-wire mesh plate. The flame was ignited and stabilized before the sample was inserted at the center of the flame. In some experiments,

**Fig. 2** Schematic of an optical single-particle burner, adapted from [18] (Color figure online)



the thermocouple was removed after the temperature remained stable, to avoid damaging the thermocouple due to the excessive heat produced during volatile combustion. The chamber was at atmospheric pressure. A 3CCD camera (CV-M9 GE JAI) at a frequency of 30 Hz recorded the morphological change in the sample (Fig. 2).

## Results

### Effect of Particle Size on Conversion at Different Residence Times

The combustion of particles at the two residence times of 0.47 and 0.65 s were studied in the DTF. The products after the test included soot, tar, solid residue, and gas. PUR, transparent PE, and SRM were tested. The only material that reacted during the tests was SRM. Figure 3 shows the solid residue yield for SRM at each particle size for the two residence times. Solid residue was calculated based on the ratio of the mass of the solid residue after the test to the mass of the original particle. The weight loss of the particles in the furnace corresponds to the extent of particle conversion. No significant amount of tar or soot was observed during these experiments. At the particle size of 7 mm, there was no weight loss at either of the two residence times. At the shorter residence time, the solid residue yield was higher, which indicates that less conversion took place.

No significant change in the weight of the particles was observed at both residence times for PUR and PE at all particle sizes. The residence time of particles in this furnace is not long enough to start the conversion. To study the conversion of these plastic materials with respect to time, the optical single-particle burner was used.

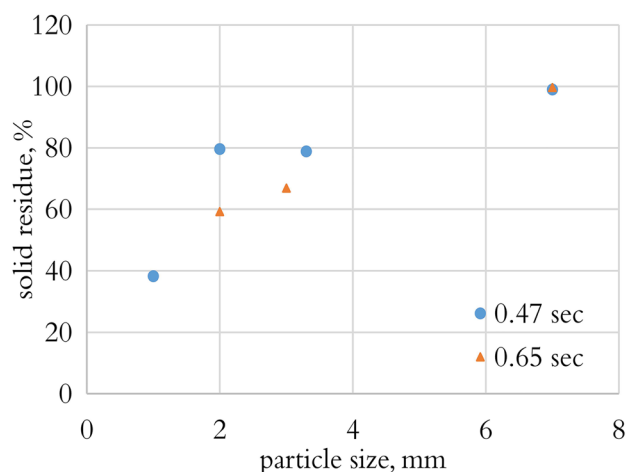


**Fig. 3** Solid residue yields at two residence times for SRM of different particle sizes at 1250 °C (Color figure online)

### Visual Observations During Particle Conversion

Figure 4 shows an example of the phenomenon that was observed during conversion of the samples in the optical single-particle burner. Particles went through ignition, devolatilization, and char combustion steps. To identify each of these steps during the conversion in the OSB, the following definitions are used:

- **Ignition time:** the duration between the moment when the sample is inserted into the center of the chamber and the moment of the first appearance of a visible flame. In the case where samples start to ignite before reaching the center, the ignition time is reported as negative.
- **Devolatilization time:** the duration between the ignition time and the moment with the last visible flame.

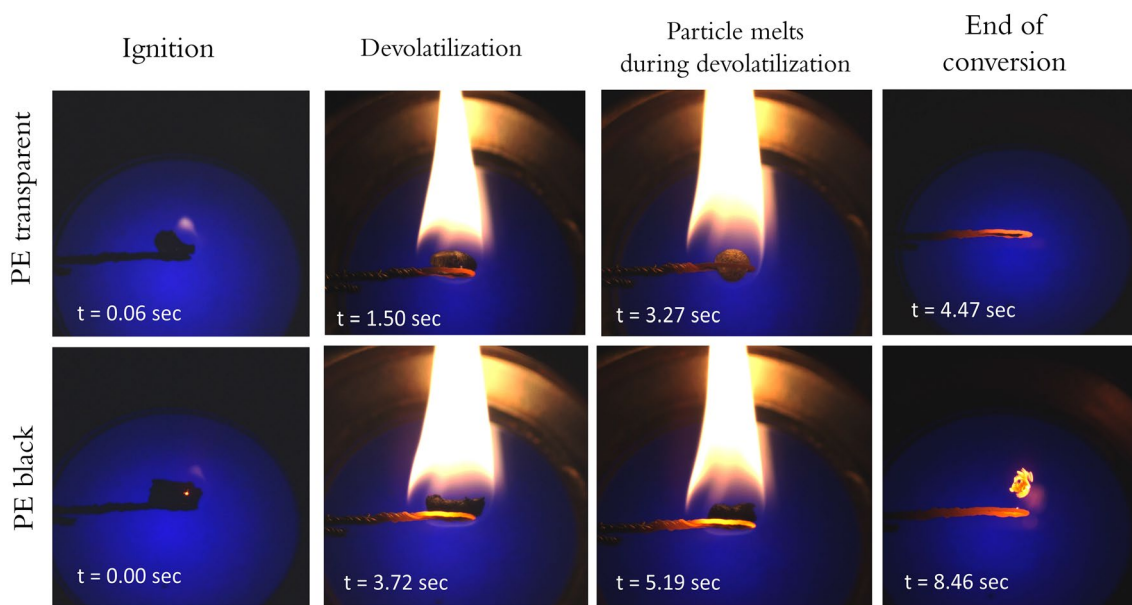


**Fig. 4** Example of recorded images during conversions of transparent PE and black PE (3 mm); the temperature was set to 1250 °C (Color figure online)

The remaining material is char and/or ash. Particles may swell or shrink during devolatilization

- **Char combustion time:** the duration after the extinction of the visible flame and the termination of the char particle combustion process. The existence of the char combustion process was judged by light emission from the particle. The remaining particle after devolatilization (char) can continue to shrink until it stops reacting and only ash remains. The ash could remain or fly away.
- **Total conversion time:** the sum of ignition, devolatilization, and char burnout times. By the end of this time, the particle is fully converted.

Figure 4 shows the change in morphology of both transparent and black PE during conversion. During devolatilization, the transparent PE particles appeared to have melted and transformed into a spherical shape, with bubbles forming inside the particle (Fig. 5a). However, due to signal interference from the flame, it was difficult to determine the change in the diameter of the particle. During the devolatilization of transparent PE, some particles were observed to have flown through the flame, which suggests that the particle transforms to fragments during conversion (Fig. 5b). The particle completely disappears once devolatilization stops and the flame also disappears. In other words, the particle was converted by devolatilization alone, and no char oxidation was observed.

The black PE particles showed similar behavior to that of the transparent PE particles (Fig. 4, PE black), except that

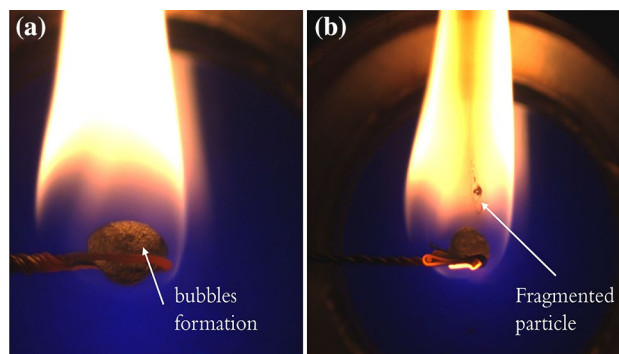


**Fig. 5** a Bubble formation inside transparent PE, b soot formation observed in the flame (Color figure online)

after devolatilization stops, a small solid residue remained that flew away. This suggests that the particle produces a light char that is carried away by the gas flow. The black PE particles melted during conversion; however, fragmentation was not observed.

Figure 6 shows that the PUR particle was ignited as soon as it was inserted into the chamber. During the PUR devolatilization, a fume was observed within the flame, which is probably suggestive of the detachment of material from the particle (Fig. 7a). PUR swelled during the devolatilization. At the end of devolatilization, material deposition was observed at top of the particle (Fig. 7b). Unlike PE, PUR produced char after devolatilization, which continued to glow and shrink. Finally, the particle stopped glowing, and

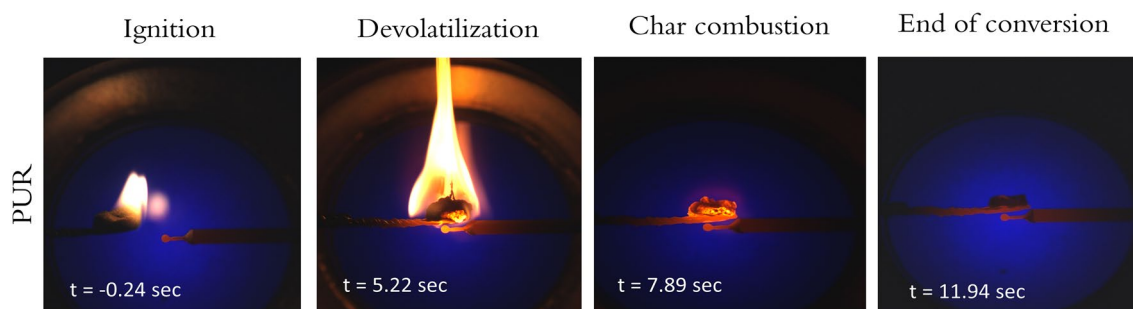


**Fig. 6** Examples of recorded images during conversion of PUR (2 mm); the temperature was set to 1250 °C (Color figure online)

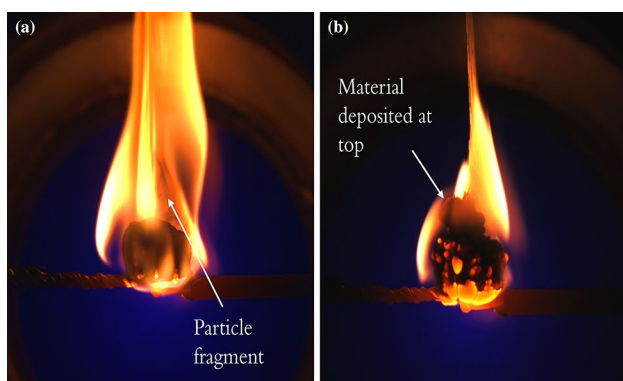


**Fig. 7** **a** Particle fragmentation during PUR devolatilization, **b** material deposition formed on top of particle (Color figure online)

the particle size remained the same. The ash that remained after combustion had the same cylindrical shape as the original PUR, though with a smaller diameter.

SRM consists of different types of plastic materials, and thus, its conversion characteristics are varied. Figure 8 shows three examples of SRM particles with different conversion characteristics. Particle 1 in Fig. 8 shows that the particle swelled until the end of devolatilization ( $t=4.98$  s). Once the devolatilization was complete, the particle continued to shrink due to char combustion. No visible flame was observed during the conversion of particle 2 (Fig. 8). The particle shrank rather than swelled during the combustion until it disappeared.

The flame that was observed during the devolatilization of the third particle did not show a uniform shape, which could be due to a different pore opening of the particle. The particle size was smaller than the initial size upon completion of the devolatilization ( $t=7.14$  s). The particle continued to shrink until it stopped glowing. These are just a few examples of some of the conversion characteristics observed for SRM, and a variety of other conversion characteristics were also observed. Some particles only converted by devolatilization,

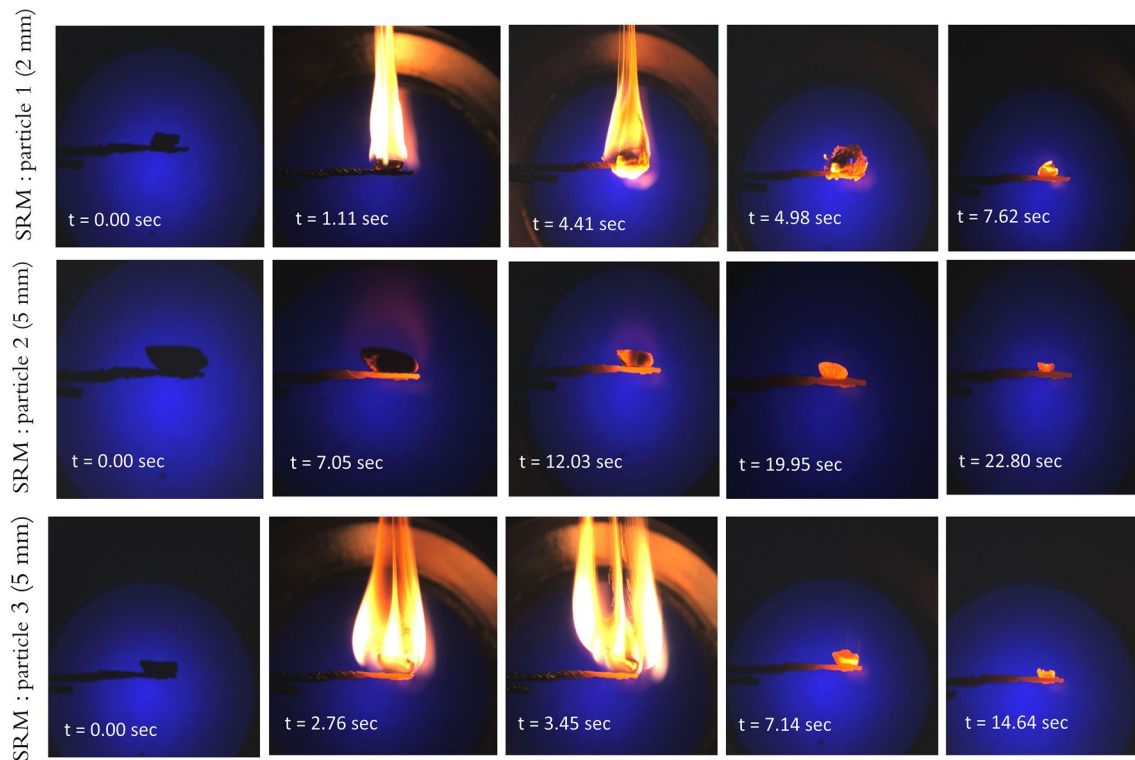
while some produced char and went through char combustion as well.

The coal sample was in the pulverized form as it is normally used in the fuming process. Thus, it was not possible to perform the experiment with the platinum wire that was used for the single plastic particles. Instead, the wire was inserted into the coal powder, and as a result, a pack of particles was collected on the wire. Thus, the conversion characteristics were not measured for single coal particles, rather, for a cluster of more particles as shown in Fig. 9. A flame was observed during devolatilization. After char combustion, a light ash remained, which flew away. The conversion of coal was mainly determined by the char combustion time, while for plastic materials, devolatilization was the main conversion stage. The devolatilization time of coal was 1.83 s, and the total conversion time was 16 s.

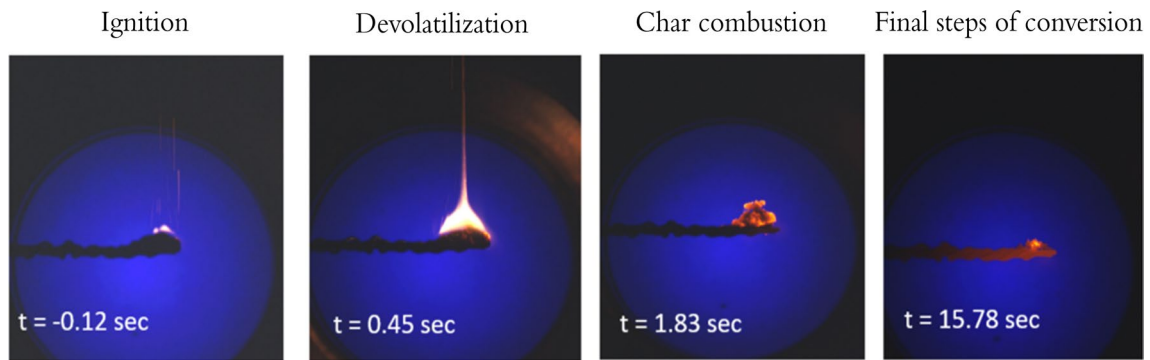
### Effect of Particle Size on Conversion Time of Different Samples

Figure 10 shows the ignition, devolatilization, and char combustion times for all tested materials with different particle sizes. The standard deviation was insignificant for all the plastic materials studied except for SRM, and only the mean values are presented. The devolatilization times of transparent PE and black PE particles were similar. The devolatilization times of both PE particles, black and transparent, increased as the particle size increased, though not linearly. In the case of PUR (Fig. 10c), the devolatilization and the char combustion time also increased with the increasing particle size, while the ignition time remained approximately the same. The increase in devolatilization time was not linear. The devolatilization time of PUR was longer than that of PE with the corresponding particle size. The average devolatilization and char combustion times, and the standard deviations for the SRM are presented in Fig. 10d. As the particle size increased, the devolatilization time also increased.

Another important parameter, apart from the time required for each phenomenon occurring during conversion, is the total time needed for conversion. Figure 11 shows



**Fig. 8** Examples of images recorded during conversion of different SRMs of different particle sizes; the temperature was set to 1250 °C (Color figure online)



**Fig. 9** Observations during the conversion of packed coal particles; the temperature was set to 1250 °C (Color figure online)

the total conversion times for all tested materials with different particle sizes. PE had the shortest total conversion time, and PUR had the longest total conversion time among the plastic-containing materials. As SRM showed a variety of conversion times, the average total conversion time is reported. At each particle size, the conversion time of SRM was longer than that for PE.

## Discussion

Injection of the reductant with air to the furnace leads to a plume formation in front of the tuyeres. Reductant particles are subject to oxidizing conversion as they pass through the plume. Conversion process includes ignition, devolatilization, volatile combustion, and char combustion. The extent of conversion depends on the residence time of the particles in the plume, which in turn is dependent on the plume

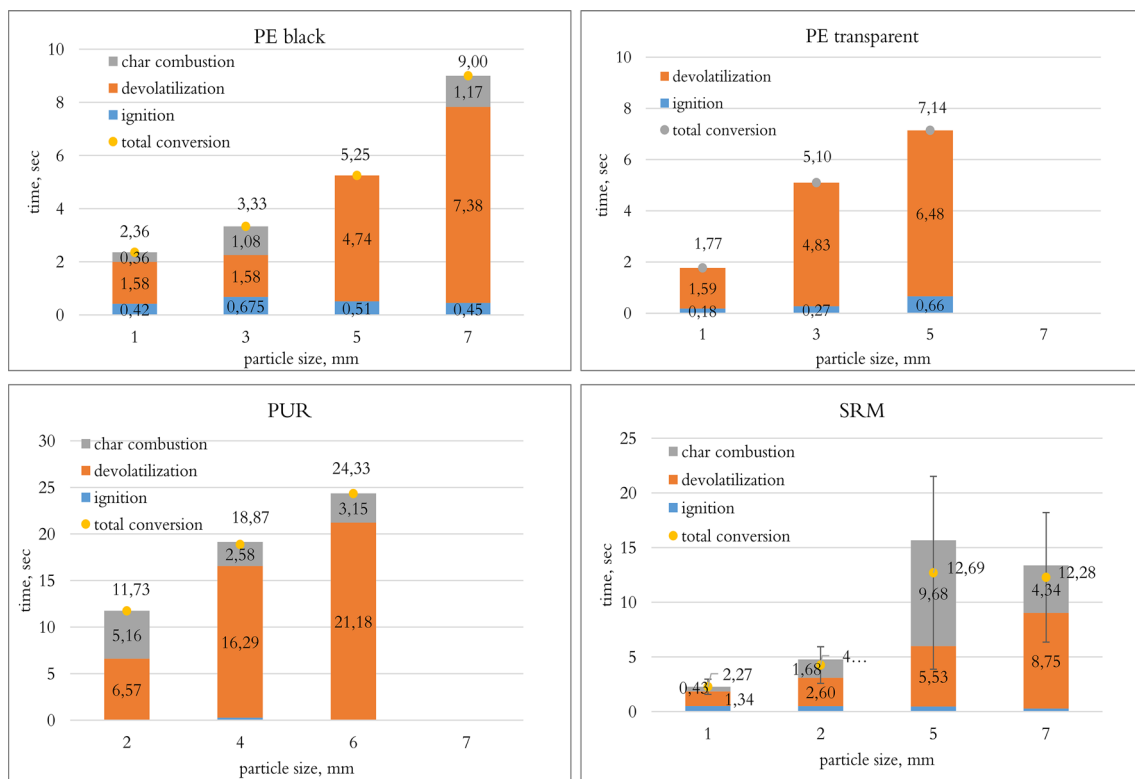


**Fig. 10** Ignition, devolatilization, and char combustion times for tested samples of different particle size at 1250 °C. The standard deviation is only demonstrated for SRM, as the standard deviation was negligible for the remaining materials (Color figure online)

diameter and the velocity of the particles. Determination of the change in the plume size or the velocity of the particles due to change of the reductant to plastic materials, is beyond the scope of this article. Thus, the only parameter considered and measured is the conversion characteristics of the particles. Both black and transparent PE particles have shorter conversion times compared with PUR; thus, under similar residence times in the plume, PE will convert more than PUR. The difference in conversion characteristics of these two plastic materials is due to differences in their structure. PE consists of ethylene chains, which break down by random session without producing char. PUR, on the other hand, consists of aromatic rings, which can recombine and produce char [19]. As a result, char combustion elongates the total conversion time of PUR. SRM consists of a variety of plastic materials, such as polypropylene (PP), which, similar to PE, do not produce char during conversion. SRM also consists of plastics, such as polyvinyl chloride (PVC), which do produce char during conversion [20]. For this reason, SRM demonstrates numerous conversion times; therefore, the extent of SRM conversion in the plume varies.

The total conversion time of the plastic materials studied here, at the smallest particle size, is in the order of seconds, while the conversion time of the currently used reducing agent, pulverized coal, is reported to be in the order of

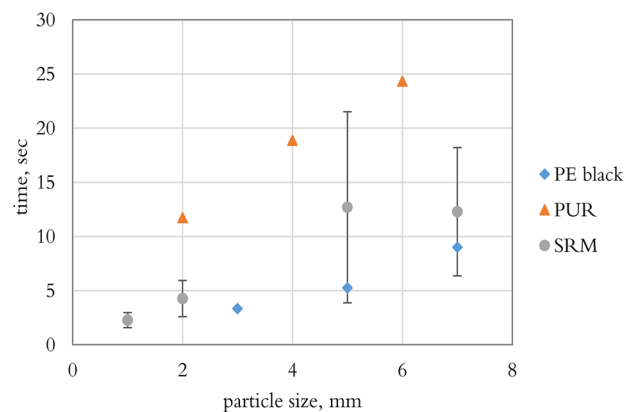


**Fig. 11** Total conversion times for the tested materials with different particle sizes (Color figure online)

milliseconds. Timothy et al. [21] studied the total combustion time for single coal particles with particle size of 38–45 μm and reported that the total combustion time is between 20 and 40 ms. Thus, the studied plastic materials would be converted less in the plume compared with coal. However, for all plastic materials with a smaller particle size, a shorter conversion time was observed. Thus, the decrease in particle



size would possibly improve the conversion rate of plastic materials.

In this study, the conversion time of packed coal particles was studied, which showed a total conversion time of 16 s. Other researchers [5] mentioned the tendency of coal particles to agglomerate during injection. The agglomerated coal particles would be similar to the packed coal particles. The packed particles required a considerably longer time to convert compared with single particles; hence, it is possible that the fraction of coal that would agglomerate does not fully convert during the process.

Zinc fuming is controlled by the contact between ZnO and the reducing gases in the slag bath. Reducing gases can be produced by combustion of the reductant in the tuyere, and they can be further detached from the plume in bubble form. In addition, reductant particles can penetrate and be converted in the slag bath. In this case, the reductant will probably be surrounded by volatiles forming a bubble, and the efficiency of the reducing agent would be dependent on the residence time of the formed bubble. For an alternative reducing agent to be efficient, its conversion time should be shorter than the residence time of the formed bubble. The residence time of the bubble is dependent on the bubble's diameter and its motion in the fuming bath. Plastic materials contain a higher concentration of volatiles and a larger particle size; thus, they are expected to generate a larger bubble. Larger bubbles have a lower residence time in the slag, which decreases the reduction efficiency. Although the relationship between the plastic particle size and the bubble size is not clear, at these particle sizes, the plastic materials tested will probably create larger bubbles compared with coal, which could possibly reduce their efficiency.

Another parameter to consider is the composition of gases within the bubble. The gases generated through conversion are more likely to consist of CO and CO<sub>2</sub>, while the gases produced through the devolatilization of the plastic materials are mainly hydrocarbons. The hydrocarbons formed need to break into C and H<sub>2</sub> in order to be able to participate in reduction, which is known to be a slow process [22]. Thus, it is possible that with the slow decomposition of hydrocarbons, the residence time of the bubble is not long enough to complete the hydrocarbon cracking.

Finally, no significant conversion was observed for PE and PUR in the DTF, while devolatilization of the particles was started in the OSB burner at corresponding residence times. This could be due to the different dominant heat-transfer mechanisms between these methods. Radiation is the dominant heat-transfer mechanism in the DTF test, while convection is the main mechanism of heat transfer in the OSB. Correspondingly, the dominant heat-transfer mechanisms in the plume and slag bath could be different, which could lead to a difference in the conversion time.

In conclusion, to select a possible alternative reducing agent, the conversion characteristics of particle and bubble residence times are important. Both these parameters are dependent upon the operational conditions in the furnace, such as slag chemistry and the injection system.

## Conclusions

Conversion characteristics of plastic-containing materials under oxidizing conditions as possible alternative reducing agents were studied, and were compared with the currently used reducing agents. The effect of particle size on conversion characteristics was studied using a single-particle optical burner and a drop tube furnace. The following conclusions have been drawn:

- PE has the shortest conversion time among the studied materials. PE conversion occurs mainly by devolatilization.
- PUR has the longest conversion time, and during conversion, both devolatilization and char combustion take place. SRM shows a variety of conversion characteristics, and thus, various conversion times.
- For all plastic materials tested, for a smaller particle size, a shorter conversion time was observed.
- No conversion was observed for transparent PE and PUR tested in the drop tube furnace. The extent of conversion for SRM was different in the DTF from the one for the OSB at similar residence times. This is probably due to the different heat-transfer mechanisms in these two furnaces.
- The conversion times for all plastic materials tested with the studied particle sizes are longer than the reported conversion time for coal when used as a reductant in the fuming processes.

**Acknowledgements** The financial contributions from, Boliden Commercial, Vinnova-supported strategic innovation program for the Swedish mining and metal producing industry; SIP STRIM; Stena International Recycling; and Kuusakoski Sverige AB, are gratefully acknowledged. The study was conducted and to a lesser extent financed—within the context of CAMM (Center of Advanced Mining and Metallurgy) at the Luleå University of Technology. The helps from Albert Bach and Carl Bormann for conducting the experiments are greatly acknowledged.

## Compliance with Ethical Standards

**Conflict of interest** On behalf of all the authors, the corresponding author states that there is no conflict of interest.

**Open Access** This article is distributed under the terms of the Creative Commons Attribution 4.0 International License (<http://creativecommons.org/licenses/by/4.0/>), which permits unrestricted use, distribution, and reproduction in any medium, provided you give appropriate credit to the original author(s) and the source, provide a link to the Creative Commons license, and indicate if changes were made.

## References

- Cui J, Forssberg E (2003) Mechanical recycling of waste electric and electronic equipment: a review. *J Hazard Mater* 99(3):243–263
- Schlummer M, Mäurer A, Leitner T, Spruzina W (2006) Report: recycling of flame-retarded plastics from waste electric and electronic equipment (WEEE). *Waste Manag Res* 24(6):573–583
- Menad N, Björkman B, Allain EG (1998) Combustion of plastics contained in electric and electronic scrap. *Resour Conserv Recy* 24(1):65–85
- Lotfian S, Vikström T, Björkman B, Lennartsson A, Ahmed H, Samuelsson C; Plastic-containing materials as alternative reductants for base metal production. *J Can Metall Q*
- Richards GG, Brimacombe JK, Toop GW (1985) Kinetics of the zinc slag-fuming process: Part I: Industrial measurements. *Metall Trans B* 16(3):513–527
- Huda N, Naser J, Brooks GA, Reuter MA, Matuszewicz RW (2012) Computational fluid dynamics (CFD) investigation of submerged combustion behavior in a tuyere blown slag-fuming furnace. *Metall Mater Trans B* 43(5):1054–1068
- Ghosh B, Orning AA (1955) Influence of physical factors in igniting pulverized coal. *Ind Eng Chem* 47(1):117–121
- McLean WJ, Hardesty DR, Pohl JH (1981) Direct observations of devolatilizing pulverized coal particles in a combustion environment. In: *Symposium (International) on Combustion* 18(1):1239–1248
- Kaminsky W, Predel M, Sadiki A (2004) Feedstock recycling of polymers by pyrolysis in a fluidized bed. *Polym Degrad Stabil* 85(3):1045–1050
- Woolley WD, Fardell PJ (1977) The prediction of combustion products. *Fire Saf J* 1(1):11–21
- Conesa JA, Font R, Marcilla A, Garcia AN (1994) Pyrolysis of polyethylene in a fluidized bed reactor. *Energy Fuels* 8(6):1238–1246
- Singh H, Jain AK (2009) Ignition, combustion, toxicity, and fire retardancy of polyurethane foams: a comprehensive review. *J Appl Polym Sci* 111(2):1115–1143
- Zevehoven R, Karlsson M, Hupa M, Frankenhaeuser M (1997) Combustion and gasification properties of plastics particles. *J Air Waste Manag* 47(8):861–870
- Alston SM, Clark AD, Arnold JC, Stein BK (2011) Environmental impact of pyrolysis of mixed WEEE plastics part 1: experimental pyrolysis data. *Environ Sci Technol* 45(21):9380–9385
- Hall WJ, Williams PT (2006) Fast pyrolysis of halogenated plastics recovered from waste computers. *Energy Fuels* 20(4):1536–1549
- Umeki K, Häggström G, Bach-Oller A, Kirtania K, Furusjö E (2017) Reduction of tar and soot formation from entrained-flow gasification of woody biomass by alkali impregnation. *Energy Fuels*. 31(5):5104–5110
- Molinder R, Wiinikka H (2015) Feeding small biomass particles at low rates. *Powder Technol* 269:240–246
- Bach-Oller A, Furusjö E, Umeki K (2015) Fuel conversion characteristics of black liquor and pyrolysis oil mixtures: efficient gasification with inherent catalyst. *Biomass Bioenerg* 79:155–165
- Beyler CL, Hirschler MM (2002) Thermal decomposition of polymers. In: *SFPE handbook of fire protection engineering*, Springer, New York
- Martinho G, Pires A, Saraiva L, Ribeiro R (2012) Composition of plastics from waste electrical and electronic equipment (WEEE) by direct sampling. *Waste Manag* 32(6):1213–1217
- Timothy LD, Sarofim, AF, Beér, JM (1982) Characteristics of single particle coal combustion. In *Symposium (International) on Combustion* 19(1):1123–1130
- Quarm TAA (1968) Slag fuming of zinc kinetic or thermodynamic. *Eng Min J* 169(1):92–93